High-fructose diet downregulates long-chain acyl-CoA synthetase 3 expression in liver of hamsters via impairing LXR/RXR signaling pathway[s]

Bin Dong, Chin Fung Kelvin Kan, Amar B. Singh, and Jingwen Liu[1]

Department of Veterans Affairs, Palo Alto Health Care System, Palo Alto, CA 94304

Abstract   Long-chain acyl-CoA synthetases (ACSL) play key roles in fatty acid metabolism in liver and other metabolic tissues in an isozyme-specific manner. In this study, we examined the effects of a fructose-enriched diet on expressions of ACSL isoforms in the liver of hamsters. We showed that the fructose diet markedly reduced the mRNA and protein expressions of ACSL3 in hamster liver without significant effects on other ACSLs. The decrease in ACSL3 abundance was accompanied by a reduction in ACSL-catalyzed synthesis of arachidonyl-CoA and oleoyl-CoA in liver homogenates of hamsters fed the fructose diet as opposed to normal diet. We further showed that fructose diet specifically reduced expressions of three key components of the LXR signaling pathway, namely, liver X receptor (LXR)α, LXRβ, and retinoid X receptor (RXR)β. Exogenous expression and activation of LXRα/β increased hamster ACSL3 promoter activities in a LXR-responsive element (LXRE)-dependent fashion. Finally, we showed that treating hamsters with LXR agonist GW3965 increased hepatic ACSL3 expression without affecting other ACSL isoforms. Furthermore, the ligand-induced increases of ACSL3 expression were accompanied with the reduction of hepatic triglyceride levels in GW3965-treated hamster liver. Altogether, our studies demonstrate that fructose diet has a negative impact on LXR signaling pathway in liver tissue and reduction of ACSL3 expression/activity could be a causal factor for fructose-induced hepatic steatosis.—Dong, B., C. F. K. Kan, A. B. Singh, and J. Liu. **High-fructose diet downregulates long-chain acyl-CoA synthetase 3 expression in liver of hamsters via impairing LXR/RXR signaling pathway.** *J. Lipid Res.* **2013.** 54: **1241–1254.**

Supplementary key words   gene expression • liver X receptor • retinoid X receptor

The liver has a central role in the control of whole-body lipid metabolism by regulating the uptake, synthesis, oxidation, and export of lipids to adapt to the needs of the organism under different nutritional environments. This adaptation requires major changes in the hepatic metabolic gene program. One gene family, long-chain acyl-CoA synthetase (ACSL), encodes enzymes that play key roles in lipid metabolism in liver, as well as other metabolic tissues (1–5). ACSL catalyzes the formation of fatty acyl-CoA from ATP, CoA, and long-chain fatty acids (FAs). This reaction is the first step in FA metabolism following transport of nonesterified FA into mammalian cells. This activation process is essential for cellular utilization of FA via different metabolic pathways, including the cellular β-oxidation system responsible for FA oxidation (catabolism) and the anabolic pathways for the synthesis of phospholipids, cholesterol esters, and triglycerides (TG). To date, five isoforms of ACSL (ACSL1, ACSL3, ACSL4, ACSL5, and ACSL6) have been characterized in humans, mice, and rats (3). These isoforms differ considerably in their characteristics, including substrate specificity, enzyme kinetics, and tissue and subcellular distribution. These individual characteristics contribute to their different cellular functions and metabolic outcomes (6–14). Because each isoform of the ACSL family has a distinct function in directing acyl-CoA to one or more specific downstream pathways, the level of expression/activity of individual ACSL isozymes could directly influence FA metabolic fates in liver tissue.

Nutritional status and hormone levels differently affect the gene expression of ACSL family members in liver tissue (15–17). In mice fed a normal chow diet, fasting increased the mRNA abundance of ACSL4 and ACSL1 in the liver, and fasting decreased ACSL3 and ACSL5 mRNA levels. In liver of Wister rat, fasting had little effect on ACSL5 mRNA expression, but refeeding markedly increased

Abbreviations: AA, arachidonic acid; ACSL, long-chain acyl-CoA synthetase; EMSA, electrophoretic mobility shift assay; FD, fructose diet; LXR, liver X receptor; LXRE, LXR response element; ND, normal diet; OA, oleic acid; PA, palmitic acid; PPAR, peroxisome proliferator-activated receptor; PPRE, PPAR-responsive element; RXR, retinoid X receptor; TC, total cholesterol; TG, triglyceride.

[1] To whom correspondence should be addressed.
  e-mail: Jingwen.Liu@va.gov

[s] The online version of this article (available at http://www.jlr.org) contains supplementary data in the form of two figures.

both ACSL5 mRNA and protein levels. Although the mechanisms that regulate transcriptions of ACSL isoenzymes by diets are not fully understood, it has been shown that class II nuclear receptors, particularly members of the peroxisome proliferator-activated receptors (PPAR), are involved in the regulation of ACSL transcription. Two earlier reports provided initial evidence for the PPARα-mediated induction of ACSL1 mRNA in rat hepatocytes, mouse Fa-32 hepatoma cells, and rat liver (18, 19). Another study reported that treating rats with a potent PPARγ-specific ligand increased expression of ACSL1 mRNA in muscle and adipose tissue, but not in liver or heart (20). Additionally, it was shown that, in rats, the PPARα agonist, GW9578, elevated hepatic mRNA levels of ACSL1 and ACSL4 without altering ACSL5 mRNA levels (6). Our other studies have identified PPARδ as an important transactivator for the hepatic expression of ACSL3 via two PPAR-responsive elements (PPRE) located in the ACSL3 promoter region −944 to −915 relative to the transcription start site (21). By utilizing PPARδ-specific agonist L165041, we further demonstrated that activation of PPARδ led to increases in ACSL3 mRNA level and protein level in HepG2 cells as well as in hamster liver. Collectively, these studies suggest that the gene expressions of ACSL isozymes are subject to regulation by common or specific members of the PPAR family in a tissue-specific manner.

Liver X receptors (LXR) also belong to the class II nuclear receptor subfamily (22, 23). The LXR family consists of two subtypes, LXRα and LXRβ. LXRs form obligate heterodimers with retinoid X receptor (RXR), which has three isotypes, RXRα, RXRβ, and RXRγ (24). LXR-RXR heterodimers regulate gene transcription via direct binding to LXR response elements (LXRE) located in promoter regions of their target genes. LXREs consist of direct repeats of the consensus half-site sequence 5′-AGGTCA-3′, in which the half sites are spaced by four nucleotides, referred to as a DR4 motif. Both isoforms of LXRα and LXRβ and the RXR isoforms α and β are expressed in the liver, where they play important roles in the regulation of cholesterol homeostasis. Activation of LXRs by endogenous ligands of oxidized cholesterol derivatives and pharmaceutical agonists leads to induction of genes involved in reverse cholesterol transport and mobilization of cholesterol, such as the ATP binding cassette (ABC) transporter genes ABCA1, ABCG1, ABCG5, and ABCG8, and genes involved in bile acid synthesis, such as CPY7A (25, 26). Interestingly, a recent report has shown that treating placental trophoblast cells with LXR synthetic ligands stimulated ACSL3 gene transcription, and this effect was mapped to a LXRE motif located 163 bp upstream of the transcription start site (27), which is downstream of PPRE sites. This study further showed that in cultured human placental BeWo cells, in addition to ACSL3, ACSL5 and ACSL6 were induced by an LXR agonist, implying that these three ACSL isozymes could all be the downstream targets of LXR signaling pathways (27).

The golden Syrian hamster has been used with increasing frequency in recent years to study lipoprotein metabolism and atherosclerosis and to evaluate the effects of hypolipidemic agents, including PPAR agonists (28, 29), because hamsters share more characteristic features in lipid metabolism with those found in humans than mouse or rat (30–32). However, in the past, hamsters rarely had been used as in vivo models to study ACSL enzymes, and most animal studies of the acyl-CoA synthetases were carried out in mice and rats. Interestingly, by cloning hamster homolog of ACSL3 and generating anti-hamster ACSL3 antibody, we have found that the expressions of ACSL3 mRNA and protein were substantially higher in liver of hyperlipidemic hamsters than in that of normolipidemic hamsters (16). This observation made in hamsters has not been reported in mice or rats.

Mounting evidence has shown that fructose-enriched diet induces metabolic syndrome, including insulin resistance, hypertension, hyperlipidemia, and hepatic steatosis in animal models (33, 34). Although to a lesser extent, high-fructose intake has been shown to cause dyslipidemia and to impair insulin sensitivity in humans. Inductions of hepatic de novo lipogenesis, lipotoxicity, oxidative stress, and hyperuricemia have all been proposed as underlying mechanisms for these deleterious metabolic effects of fructose diet (35). At the molecular level, fructose diet has profound impact on the expression of genes with products critically involved in carbohydrate and lipid metabolism (36, 37). However, no study has been performed to examine whether the hepatic expressions of ACSL isoforms are altered by fructose diets.

In this study, we examined the mRNA and protein expressions of ACSL isozymes (ACSL1, ACSL3, ACSL4, and ACSL5) in liver tissues of hamsters fed a normal diet (ND) or a diet that contains 60% fructose (FD). Our results revealed for the first time that fructose diet specifically repressed ACSL3 expression without effects on other liver-expressed ACSL isoforms. By conducting in vitro and in vivo studies, we further elucidated the underlying mechanism by which fructose diet inhibits ACSL3 transcription via impairing the LXR signaling pathway.

MATERIALS AND METHODS

Animal diets

Male Syrian golden hamsters with body weights of 100–120 g were purchased from Harlan. Hamsters were housed (two animals/cage) under controlled temperature (72°F) and lighting (12 h light/dark cycles). Animals had free access to autoclaved water and food. Hamsters had a seven-day acclimation period before experiments. For the first in vivo study of fructose diet, six hamsters were switched to a high-fructose diet (60% fructose; Dyets Inc., Bethlehem, PA) for 28 days to induce dyslipidemia (29). The control hamsters (n = 6) were fed a rodent normal chow diet. At the experimental termination, after a 16 h fasting, hamsters were anesthetized, and terminal blood samples were obtained via cardiac puncture. Livers were immediately removed, cut into small pieces, and stored at –80°C for RNA isolation, protein isolation, hepatic lipid measurement, and ACSL enzyme assays.

In the second in vivo study, 32 hamsters were divided randomly into four groups having similar body weights. Groups 1 and 2 were on a normal diet and groups 3 and 4 were fed the fructose diet for two weeks. While continuous on their respective diets,

hamsters were orally dosed twice daily at 9 AM and 5 PM for seven days with either vehicle (0.5% hydroxypropyl methylcellulose in PBS, G1 and G3) or with the LXR agonist GW3965 (30 mg/kg, G2 and G4) in vehicle. GW3965 was purchased from AdooQ BioScience (Irvine, CA). During the treatment, food intake and body weight were recorded daily. At the experimental termination, after a 16 h fasting, hamsters were anesthetized, and terminal blood samples were obtained via cardiac puncture. Liver tissues were collected for RNA isolation, protein isolation, and hepatic lipid measurement.

Animal use and experimental procedures were conducted in conformity with PHS policy on humane care and use of laboratory animals and were approved by the Institutional Animal Care and Use Committee of the VA Palo Alto Health Care System.

Measurement of serum and hepatic lipid levels

Serum was isolated at room temperature and stored at $-80°C$. Extraction of lipids from liver tissues was performed as described (8). Standard enzymatic methods were used to determine total cholesterol (TC), TG, LDL-C, and HDL-C with commercially available kits purchased from Stanbio Laboratory (TX).

RNA isolation, cDNA generation, and real-time quantitative PCR

Total RNA isolation, generation of cDNA, and real-time PCR were conducted as previously reported (29). Each cDNA sample was run in duplicate. The correct size of the PCR product and the specificity of each primer pair were validated by examination of PCR products on an agarose gel. Primer sequences of hamster genes used in real-time PCR are listed in **Table 1**.

For designing hamster real-time PCR primers, if golden Syrian hamster (*Mesocricetus auratus*) mRNA sequence was available, primers were designed according to that sequence. If golden hamster mRNA sequence was not available, primers were designed according to the homologous part between the mouse (*Mus musculus*) and Chinese hamster (*Cricetulus griseus*) mRNA sequences.

Western blot analysis of ACSL and LXR/RXR in hamster liver tissues

Frozen liver tissues were homogenized in 1 ml RIPA buffer containing 1 mM PMSF and protease inhibitor cocktail (Roche). After protein quantitation using BCA protein assay reagent (Pierce), 30 μg of homogenate proteins from individual liver samples were resolved by SDS-PAGE, and ACSL isoforms were detected by immunoblotting using rabbit anti-hamster ACSL3 antibody (16), anti-human ACSL4 antibody (generously provided by Dr. Diana M. Stafforini, Huntsman Cancer Institute, University of Utah), and anti-human ACSL1 (ab76702) obtained from Abcam (Cambridge, MA). Nuclear extracts were isolated from hamster livers, and LXR/RXR isoforms were detected with individual antibodies against LXRα/β (PP-K8607-00, PP-K8917-00; R and D systems); RXRα (D-20, Santa Cruz Biotechnology); and RXRβ (#8517, Cell Signaling). For ACSL detection, the membranes were reprobed with a monoclonal anti-β-actin antibody (Clone AC-15, Sigma) to normalize differences in total protein loading. For LXR/RXR detection, the membrane was reprobed with anti-HDAC1 antibody (H-51, Santa Cruz Biotechnology) as a control of equal nuclear protein loading.

Measurement of liver acyl-CoA synthetase activity

Approximately 50 mg frozen liver tissue were dounce-homogenized 15 times in a buffer containing 250 mM sucrose, 10 mM Tris (pH 7.4), 1 mM EDTA, 1 mM dithiothreitol (DTT), protease inhibitor cocktail (Roche), and phosphatase inhibitor cocktail

(Sigma). Homogenates were centrifuged at 16,000 g for 30 min at 4°C, protein concentrations in supernatants were determined by BCA assay, and aliquots were stored at $-80°C$. Initial rates of total ACSL activity in liver homogenate were measured using 4 μg of liver homogenate at 37°C in the presence of 175 mM Tris (pH 7.4), 8 mM $MgCl_2$, 5 mM DTT, 10 mM ATP, 250 μM CoA, 50 μM [³H]palmitic acid (PA), [³H]oleic acid (OA), or [³H] arachidonic acid (AA) in 0.5 mM Triton X-100, and 10 μM EDTA in a total volume of 0.1 ml. The reaction was initiated by adding the homogenized sample and terminated by adding 1 ml Dole's reagent as previously described (21). Generated [³H]PA-CoA, [³H]OA-CoA, and [³H]AA-CoA were extracted, and the radioactivity was determined in a scintillation counter. The radioactivity in the reaction that contained all components but omitted homogenate was included as a negative control.

Cloning of hamster ACSL3 promoter and construction of luciferase reporter

Primers covering the mouse ACSL3 proximal promoter region from -128 to $+68$ relative to the transcription start site were used to amplify the hamster ACSL3 promoter sequence from hamster genomic DNA. The PCR product was sequenced, and the LXRE motif was identified by the program Transfect. The 196 bp fragment of the hamster ACSL3 proximal promoter region was first cloned into Topo 2.1 vector and then subcloned into pGL3-basic at the Kpn1 and Xho1 sites. After transformation and propagation in *E. coli*, two independent clones were sequenced to verify the sequence and orientation of the promoter fragment.

Luciferase reporter assay

Luciferase reporter assay was performed by using Firefly Luciferase Reporter Assay System (Promega) according to the manufacturer's instructions. Two independent pGL3-hamster-ACSL3 plasmids were individually transfected into HepG2 cells along with pCMV-β-galacosidase as an internal transfection efficiency control. One day after transfection, cells were treated with 5 μM of LXR ligand GW3965 or the vehicle DMSO for 24 h. Cells were lysed with 100 μl of lysis buffer of which 50 μl was used to measure firefly luciferase activities and another 50 μl was assayed for β-galacosidase (β-gal) activity. The firefly luciferase activity was normalized to β-gal activity. Triplicate wells were assays for each condition. In separate experiments, HEK293 cells were transfected with ACSL3 luciferase reporters and plasmids encoding Flag-tagged LXRα (pCMV-LXRα), LXRβ (pCMV-LXRβ), or the empty control vector (pCMV-entry). The LXRE site-mutated hamster ACSL3 reporter (LXREmu) was generated by using the QuickChange site-directed mutagenesis kit (Stratagene), and the oligonucleotides were as described in Table 1 of EMSA probes.

Electrophoretic mobility shift assays

Individual liver nuclear extracts (NE) from ND and FD fed hamsters were prepared as described (33). Wild-type and mutated oligonucleotide probes containing hamster ACSL3-LXRE motif were annealed and end-labeled with T4 polynucleotide kinase in the presence of [γ-³²P]ATP. Each binding reaction comprised 10 mM Tris (pH 7.5), 5 mM $MgCl_2$, 1 mM DTT, 50 mM KCl, 2.5% glycerol, 1 μg of poly (dI-dC), 0.05% NP-40, and 25 μg of liver nuclear extracts in a final volume of 20 μl. The nuclear extracts were incubated with 0.5 ng of ³²P-labeled probe ($1 × 10^5$ cpm) for 10 min at room temperature in the absence or the presence of 100× of unlabeled probes or with 1 μg of antibodies for super shift assay. The reaction mixtures were loaded onto a 6% polyacrylamide gel and run in 1X TGE buffer (50 mM Tris base, 400 mM glycine, 1.5 mM EDTA, pH 8.5) at 30 mA for 2 h at 4°C. Gels were dried and visualized on a PhosphoImager. The sequences

TABLE 1. Quantitative real-time PCR primer sequences and EMSA probe sequences

Gene	Accession Number	Forward	Reverse
		Hamster	
ABCA1	NM_013454, XM_003495857	AACAGTTTGTGGCCCTTTTG	AGTTCCAGGCTGGGGTACTT
ABCG1	NM_009593, XM_003504436	GAGGACCTTCCTCAGCATCA	AGGACCTTCTTGGCTTCGTT
ACOX2	NM_053115, XM_003510232	TCGGCAAAAACTTCCAAATC	GGCTGTGTATCACAAACTCCTG
ACSL1		AACAGAAAGAAGCCCAAGC	TTGGTGAGTGATCATTGCTC
ACSL3		GGGCACCATTAGTTTGCTGT	CCGCTGTCCATTTTCATCTT
ACSL4		TATGGACTGACAGAAACATG	CAACTCTTCCAGTAGTATAG
ACSL5		CCCCATCTCCACTTCTGTCTT	GTGCATTCTGTTTGGCCATAAGCT
CPT1a	AY762566	GGCCATCTGTGGGAGTATGT	ACTGTAGCCTGGTGGGTTTG
GAPDH	DQ403055	AACTTTGGCATTGTGGAAGG	GGATGCAGGGATGATGTTCT
LXRα	NM_013839, XM_003497307	GCAGGACCAGCTCCAAGTAG	ATTAGCATCCGTGGGAACAT
LXRβ	NM_009473, XM_003510892	CTTCCCCCACAAGTTCTCTG	GGCTCATCCTCTGGCTCTAA
PGC1α	NM_008904, XM_003507779	TCACACCAAACCCACAGAAA	TCTGGGGTCAGAGGAAGAGA
PPARα	AJ555631	CCTGTCTGTTGGGGATGTCAC	AGGTAGGCCTCGTGGATTCT
PPARδ	AF486582	CAGCTGCACAGACCTCTCTC	CTCCGTAGTGGAAGCCTGAG
PPARγ	AB525757	TCACAATGCCATCAGGTTTG	TCAGCGGGAAGGACTTTATG
RXRα	NM_011305, XM_003513003	TCCTTCACCAAGCACATCTG	GTCGATCAGGCAGTCCTTGT
RXRβ	NM_011306, XM_003505874	GCACAGAAACTCAGCCCATT	AGCCAAGCTCTGTCTTGTCC
		Human	
ABCA1	NM_005502	AACTCTACATCTCCCTTCCCG	CTCCTGTCGCATGTCACTCC
ACSL3	NM_004457	CCACGCCTGCGGCACATCAT	TGGTTTTCCATGCTGGCCTTGG
LXRα	NM_005693	TGCCAAAGCAGGGCTGCAAGT	CTGCACGTTGGGCCGGTCTG
LXRβ	NM_007121	GTGGACTTCGCTAAGCAAGTG	GGCTGTCTCTAGCAGCATGAT
		EMSA	
Hamster ACSL3-LXRE WT		CTCCGCAGAATGACCTATAGT AACCCCGCCCCGCC	GGCGGGGCGGGGTTACT ATAGGTCATTCTGCGGAG
Hamster ACSL3-LXRE MU		CTCCGCAGAATGAggTATAG TAAgCCCGCCCCGCC	GGCGGGGCGGGcTTACT ATAccTCATTCTGCGGAG

The nucleotides in lowercase represent mutated sequences of EMSA probe.

of electrophoretic mobility shift assay (EMSA) probes are listed in Table 1. To examine the direct binding of LXRα/β to hamster ACSL3-LXRE probe, HEK293 cells were transfected with pCMV-entry, pCMV-LXRα, or pCMV-LXRβ. Two days after transfection, nuclear extracts were prepared for EMSA and super shift.

RNA interference

Small interfering RNA (siRNA) against human LXRα (catalog # s19568), LXRβ (catlaog # s14684), Silencer negative control siRNA (catalog # AM4635), and siPORT NeoFX transfection reagent were purchased from Applied Biosystems. Transfections of siRNA into HepG2 cells were done as described (21).

Statistical analysis

Values are presented as mean ± SEM. Significant differences between diet groups and control and treatment groups were assessed by one-way ANOVA with Turkey posttest and Student t-test. $P < 0.05$ was considered statistically significant.

RESULTS

Downregulation of hepatic ACSL3 expression by fructose-enriched diet in golden Syrian hamsters

Feeding male hamsters the fructose diet for four weeks increased serum triglyceride levels by approximately 60% from 102 to 162 mg/dl ($P < 0.01$) and plasma LDL-C by 75% from 33.3 to 58.5 mg/dl ($P < 0.05$) compared with hamsters fed the normal diet (supplementary Fig. IA). The hepatic triglyceride level was 27% higher in the FD group than the ND group, suggesting an induction of triglyceride synthesis by fructose diet, but the increase did not reach a statistical significance ($P = 0.06$, two tailed) (supplementary Fig. IB). No significant differences in body weight or food intake between diet groups after fructose feeding were observed. Similarly, no significant changes in fasting glucose levels were observed.

To determine whether the fructose diet could alter the hepatic expression/activity of ACSL family members that are important in directing FA partition and utilization in liver tissue under higher metabolic burdens, we examined the mRNA levels of ACSL1, ACSL3, ACSL4, and ACSL5 in liver samples of FD hamsters and compared them to ND hamsters. Because ACSL6 is not expressed in liver tissue, we did not include this isoform in the current study. **Fig. 1A** shows that fructose diet did not affect ACSL1, ACSL4, or ACSL5 mRNA expression in liver. In contrast, we detected a significant reduction of ACSL3 mRNA abundance by approximately 57% ($P < 0.001$) in livers of FD hamsters compared with the control animals. Further analysis of ACSL protein expressions by Western blotting using antibodies that specifically recognize ACSL1, ACSL3, or ACSL4 confirmed that ACSL3 protein levels in individual liver protein extracts of the FD group were substantially
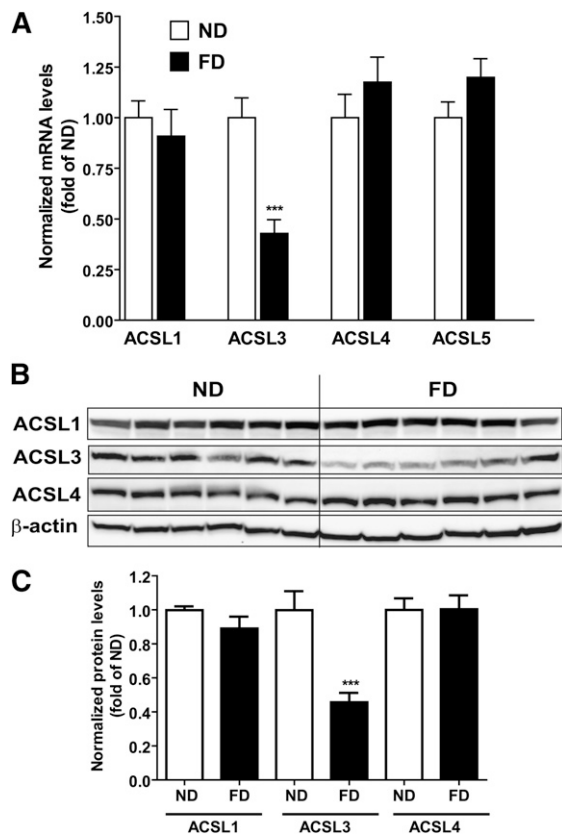
Fig. 1. Fructose diet reduces ACSL3 mRNA and protein levels in hamster liver. (A) Hamsters were fed FD or ND for four weeks. Individual levels of ACSL mRNAs were assessed by real-time qPCR using hamster-specific PCR primers as described in Materials and Methods. The relative levels presented are after normalization with GAPDH mRNA levels. Results are means ± SEM of six animals for ND group and six animals for FD group with duplicate measurement of each cDNA sample. *$P < 0.05$, ***$P < 0.001$ compared with the ND control group. (B) Individual liver protein extracts were prepared, and protein concentrations were determined. Fifty micrograms of homogenate proteins of individual liver samples were resolved by SDS-PAGE, and ACSL proteins were detected by immunoblotting using antibodies recognizing each isoform. (C) The expression levels of ACSL isoforms were quantified with Alpha View software with normalization by signals of β-actin. Values are mean ± SEM of six samples per group. ***$P < 0.001$ compared with the ND group.

lower than the normal diet group (Fig. 1B, C), whereas ACSL1 and ACSL4 protein levels were the same between the two groups. Combined with our previous observation that a cholesterol-enriched diet primarily increased ACSL3 mRNA and protein expressions in hamster liver tissue but not in other hamster tissues (16), the current results further suggest that the liver abundance of this particular isozyme of the ACSL family is highly sensitive to changes in nutrient status and is distinctively regulated by different dyslipidemic diets.

Reduction of hepatic acyl-CoA synthetase activity by fructose diet

Previous in vitro studies have suggested that purified ACSL3 has a substrate preference for C16–C20 unsaturated fatty acids (38), whereas ACSL1, the most abundant

ACSL isoform in liver, prefers saturated fatty acids such as palmitic acid. Because the individual activities of ACSL isoforms could not be distinguished, we measured total ACSL activity in liver homogenates of ND and FD in the presence of three different ^{3}H-labeled FA substrates: ^{3}H-palmitic acid (16:0), ^{3}H-arachidonic acid (20:4), and ^{3}H-oleic acid (18:1). **Fig. 2** shows that the palmitoyl-CoA synthetase activity did not differ between the two diet groups, but arachidonoyl-CoA synthetase activity and oleoyl-CoA synthetase activity in liver of FD hamsters were approximately 21.9% ($P < 0.05$) and 30.7% ($P < 0.05$) lower than that in ND hamsters, respectively. The specific reductions in arachidonoyl-CoA synthetase activity and oleoyl-CoA synthetase activity in FD liver homogenates were in line with the lower expression of ACSL3 protein in livers of FD hamsters.

Delineation of molecular pathways involved in the downregulation of hepatic ACSL3 gene expression in vivo

Our previous studies identified ACSL3 as a molecular target of PPARδ in liver cells (21). To determine whether the fructose diet reduced PPARδ expression as a causal factor for lowering ACSL3, we examined the hepatic mRNA levels of PPARδ, as well as PPARα and PPARγ, two other members of the PPAR family. Results in **Fig. 3A** show that the fructose diet did not affect PPARδ or PPARγ gene expression, but it reduced PPARα mRNA levels in FD hamster liver tissue by approximately 29% ($P < 0.05$) compared with the livers of ND hamsters. To further assess the possible effects of fructose diet on PPARα/δ activities, we measured the mRNA levels of three target genes of PPARα/δ, acyl-CoA oxidase 2 (ACOX2), carnitine palmitoyltransferase (CPT1α), and PPARγ-coactivator 1 (PGC1α). In addition, we measured the mRNA levels of ABCA1, a target gene of LXR. The results in Fig. 3B show that fructose diet did not affect mRNA expressions of these PPAR target genes. In contrast, the mRNA level of ABCA1 was reduced in FD group by approximately 40% ($P < 0.05$). To directly evaluate the function of PPARα in the hepatic expression of ACSL3 in hamsters, we treated freshly isolated hamster primary hepatocytes with different doses of PPARα agonist WY14643 for 24 h. Fig. 3C shows that activation of PPARα led to a dose-dependent increase in ACSL1 mRNA levels, which was in line with previous studies (18). In contrast, the mRNA expression of ACSL3 was unaffected. The effects of PPARα agonist on ACSL1 and ACSL3 protein expressions were further examined by Western blotting. Consistent with the results of real-time qPCR, ACSL1 protein abundance was increased by WY14643 treatment, whereas ACSL3 protein level remained the same (Fig. 3D). Altogether, these data suggested that the FD-induced downregulation of ACSL3 gene expression in liver tissue was not related to changes in PPAR expression or activity.

Next, we explored the possible role of LXR in the FD-induced repression of ACSL3 expression in hamster liver. First, utilizing real-time qPCR, we examined gene expressions of all four major components of LXR signaling pathway, including LXRα, LXRβ, RXRα, and RXRβ. **Fig. 4A** shows that the levels of three (LXRα, LXRβ, and RXRβ)
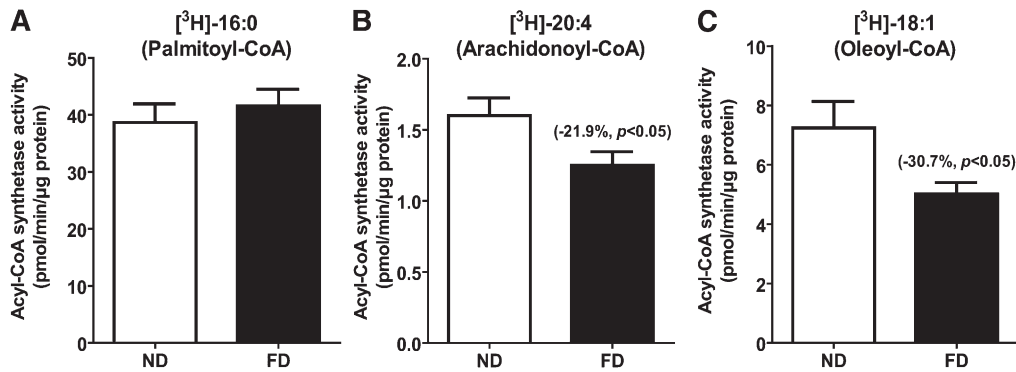
Fig. 2. Measurement of liver ACSL enzymatic activity. Initial rates of total ACSL activity in liver homogenate were measured using 4 μg of liver homogenate at 37°C in the presence of [^{3}H] labeled PA (A), [^{3}H] labeled AA (B), or [^{3}H] labeled OA (C). ND, n = 6; FD, n = 6.

out of four mRNAs were significantly reduced in livers of fructose diet as compared with those of normal diet. To confirm this finding at nuclear protein level, we isolated nuclear extracts from the frozen liver samples and performed Western blot analyses. The results shown in Fig. 4B are Western blots of individual liver samples. Quantitative analyses of the results are presented in Fig. 4C, which largely confirms the changes in mRNA expressions.

Fructose diet reduces the binding of LXR to hamster ACSL3 gene promoter

To further investigate the involvement of LXR in FD-induced downregulation of ACSL3 gene transcription, we isolated a 196 bp fragment of the hamster ACSL3 proximal promoter region that contains a sequence motif that is highly homologous to the corresponding human and mouse ACSL3-LXRE sequences (27) (**Fig. 5A**). This DNA fragment was inserted in front of the luciferase coding sequence of the pGL3-basic vector to produce the luciferase reporter construct. To determine the response of the hamster ACSL3 promoter to LXR activation, two independent reporter constructs were transfected into HepG2 cells along with β-galactosidase reporter plasmid pCMV-βGal. One day posttransfection, cells were treated with the LXR agonist GW3965 or vehicle DMSO for 24 h before cell lysis. The results of normalized luciferase assays show
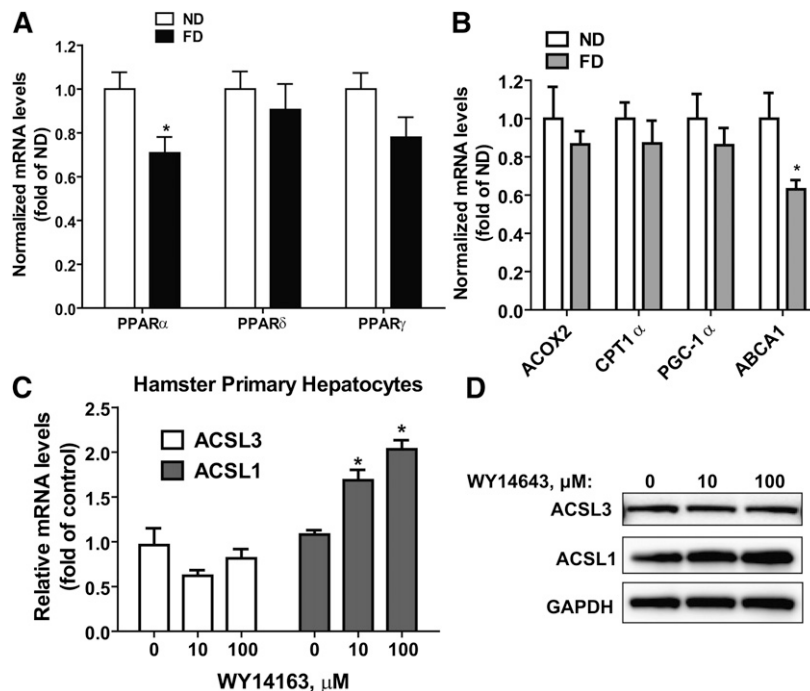

Fig. 3. Examination of the role of PPARα on modulation of ACSL3 expression in hamster liver tissue and primary hepatocytes. (A and B) Real-time qPCR assays were conducted to examine mRNA levels of PPARα, PPARδ, and PPARγ as well as PPARα/PPARδ target genes (ACOX2, CPT1α, and PGC-1α) in ND and FD liver samples. ABCA1 was included as a LXR target gene. (C and D) Hamster primary hepatocytes were cultured in HepatoZYME-SFM medium overnight. WY14643 at 10 μM and 100 μM concentrations were added to the cells for 24 h before the isolation of total RNA (C) and protein (D) for Western blotting of ACSL1 and ACSL3.
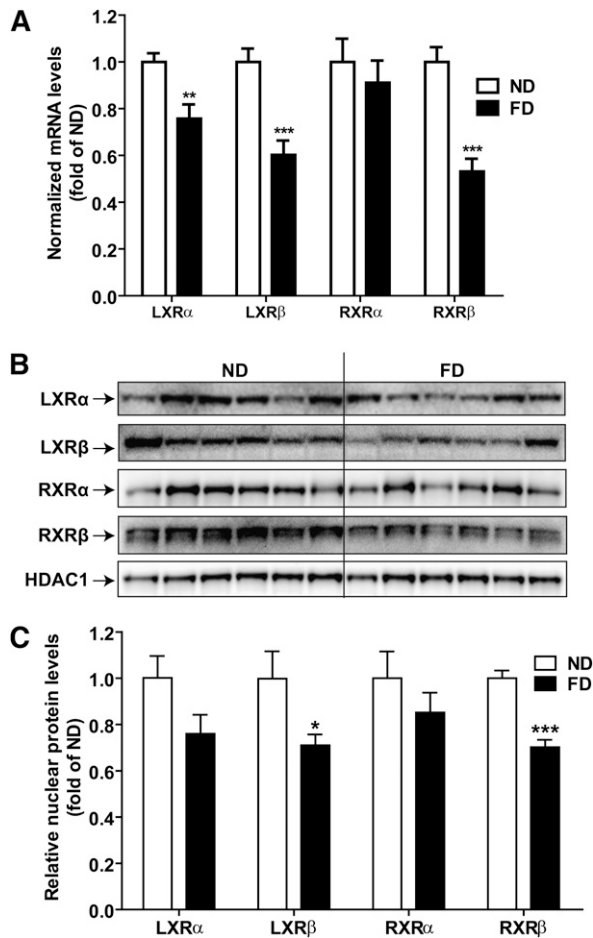
Fig. 4. Detection of fructose diet-induced changes in the expression of LXR/RXR isoforms in hamster liver. (A) Real-time qPCR assays were conducted to examine LXRα, LXRβ, RXRα, and RXRβ mRNA levels of ND and FD liver samples. (B) Six individual liver nuclear protein extracts from the ND group and from the FD group were analyzed for LXRα/β and RXRα/β protein expression by Western blotting. The membrane was reprobed with anti-HDAC1 antibody as a control of equal nuclear protein loading. (C) The protein abundances of LXR/RXR were quantified with Alpha View software with normalization by signals of HDAC1. Values are mean ± SEM of six samples per group. *$P < 0.05$ and ***$P < 0.001$ compared with the ND group.

that activation of LXR significantly increased the hamster ACSL3 promoter activity (Fig. 5B).

To further demonstrate the LXRE-dependent induction of hamster ACSL3 promoter activity by LXR activation, we mutated the LXRE site of hamster ACSL3 promoter reporter and transfected the wild-type and the mutated vectors into HEK293 cells without or with cotransfections with plasmids encoding Flag-tagged LXRα, LXRβ, or the empty control vector. The responses of ACSL3 reporters to LXR activation were assessed by treating transfected cells with 5 μM of GW3965 or its vehicle DMSO. In this set of experiments, we included human ACSL3 promoter construct (21) as a positive control. Fig. 5C clearly demonstrates that both hamster and human ACSL3 promoter activities were increased by the expression of LXRα and LXRβ. The increases were further heightened by GW3965. Mutation of LXRE site not only greatly reduced the basal

promoter activity but also completely abolished the agonist induced activation of hamster ACSL3 promoter activity. These results further confirmed the function of LXRE motif of hamster ACSL3 promoter in mediating LXR-regulated ACSL3 gene transcription in hamster species.

To detect the specific binding of LXR to the hamster ACSL3-LXRE site, we performed EMSA with a ^{32}P-labeled oligonucleotide probe (LXRE-wt) containing LXRE sequence of the hamster ACSL3 promoter and different amounts of nuclear extracts prepared from a ND hamster liver. Two complexes (C1 and C2) were detected in a dose-dependent manner (**Fig. 6A**, lanes 1 and 2). Formation of both complexes was inhibited by a 100-fold molar excess of the unlabeled wild-type oligonucleotides (Fig. 6A, lane 3), but it was not inhibited by a 100-fold molar excess of oligonucleotides containing the mutated LXRE sequence (Fig. 6B, compare lane 1 with lane 2), demonstrating the binding specificity. Next, we used equal amounts of nuclear extracts from individual liver samples from the two diet groups to compare the binding intensity. Results in Fig. 6B clearly show that the intensities of C1 and C2 complexes from FD liver samples were lower than the complex intensities of ND liver samples. These data together strongly suggest that the lesser ACSL3 expression and enzymatic activity in FD hamster liver resulted from an attenuated gene transcription owing to the reduced nuclear protein abundance of LXR isoforms.

We attempted to further characterize the protein components of C1 and C2 by conducting supershift assays with anti-LXRα or anti-LXRβ antibodies. However, the intensity of supershifted band was very weak, possibly due to the relative low affinity of the antibodies to hamster LXR proteins or the scarcity of LXRs in nuclear extracts of hamster liver samples. Thus, we transfected HEK293 cells with control vector (entry) or plasmids expressing Flag-LXRα or Flag-LXR β. Nuclear extracts were isolated from transfected cells and utilized in EMSA and supershift assays. The results in Fig. 6C show that incubation of labeled hamster ACSL3-LXRE probe with control nuclear extracts of HEK293 cells produced two weak bands that migrated in similar positions as the C1 and C2 of hamster liver nuclear extracts. Overexpression of LXRα markedly increased the intensity of these two complexes. Addition of anti-Flag antibody to the reaction mixture lowered the intensities of both bands and produced a supershifted band, whereas control antibody IgG had no effect. Exogenous expression of LXRβ slightly increased the intensity of the two complexes, and the bands were not supershifted by anti-LXRβ antibody. These results suggest that LXRα is present in both C1 and C2 and that it is the predominant protein of LXR isoforms that binds to the hamster ACSL-LXRE motif.

LXR-dependent stimulation of ACSL3 gene expression by GW3965 in liver cells in vitro

To obtain additional evidence for LXR-mediated gene transcription of ACSL3 in liver cells, we treated freshly isolated hamster primary hepatocytes with different doses of GW3965 and performed real-time q-PCR to measure
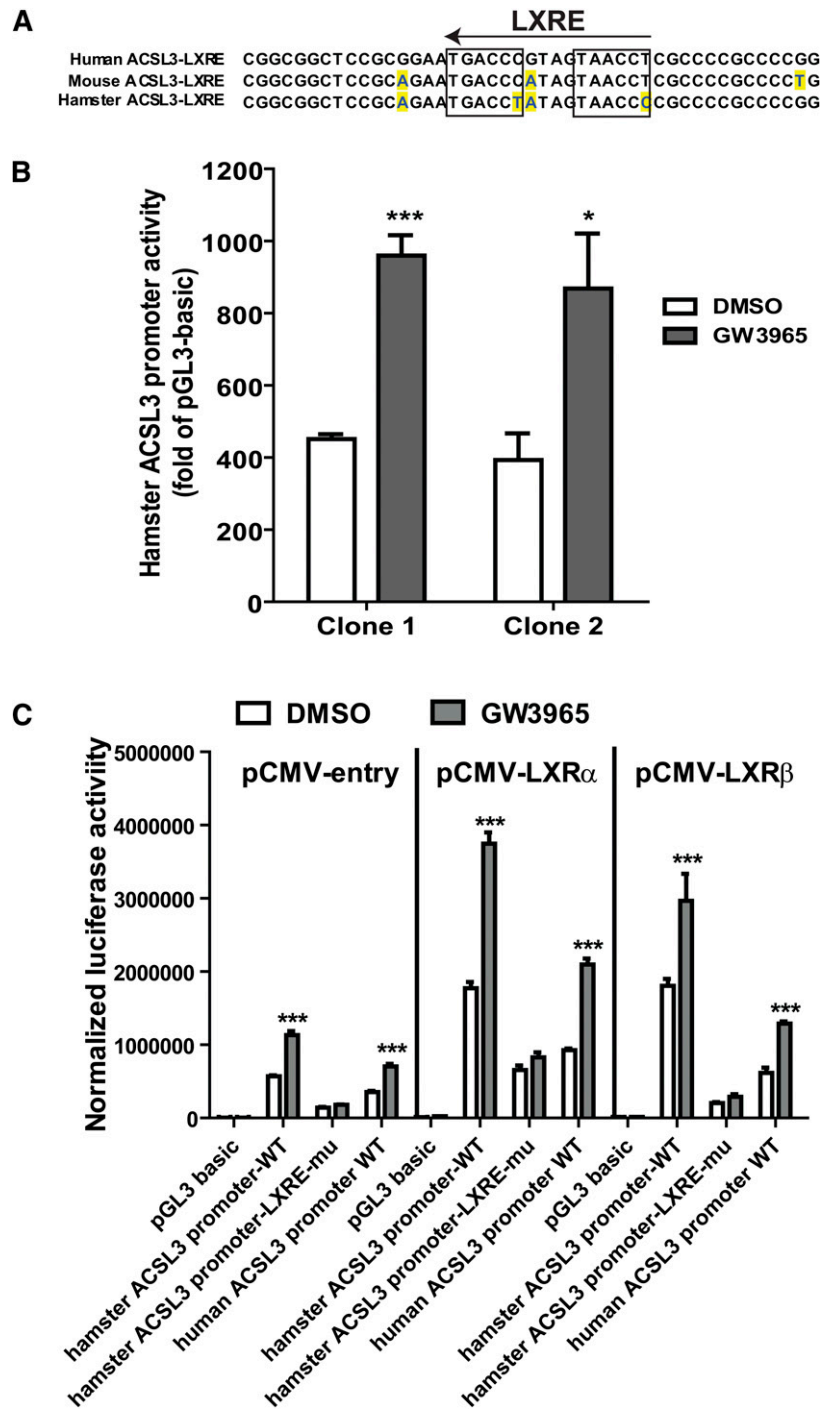
Fig. 5. Hamster ACSL3 proximal promoter contains a functional LXR binding site. (A) Scheme of proximal regions of ACSL3 promoter of human, mouse, and hamster shows the nucleotide sequences of LXRE that are located on the reverse strands of the promoters. The yellow-shaded nucleic acids represent the sequence variation from the human sequence, and the DR4 half sites are within rectangles. (B) HepG2 cells were seeded onto 96-well plates. pGL3-basic vector and two independent clones of pGL3-hamster-ACSL3 luciferase construct were cotransfected with pCMV-βGal into HepG2 cells. One day posttransfection, cells were treated with either DMSO or GW3965 at 5 μM concentration for 24 h. Cell lysates were prepared. Firefly luciferase and β-gal activities were separately measured. After normalization, ACSL3 promoter activity was expressed as the fold of pGL3-basic. Each value represents the mean ± SD of four wells per condition. *$P <$ 0.05 and ***$P <$ 0.001 compared with DMSO. (C) HEK293 cells were cotransfected with pGL3-basic, hamster ACSL3-LXRE wild-type, hamster ACSL3-LXRE-mutated, or human ACSL3 luciferase reporters and the indicated Flag-tagged expression plasmids or the control vector. One day posttransfection, cells were treated with either DMSO or GW3965 for 24 h. Cell lysates were prepared. Firefly luciferase and β-gal activities were separately measured. Normalized luciferase activity was expressed. ***$P <$ 0.001 compared with DMSO.
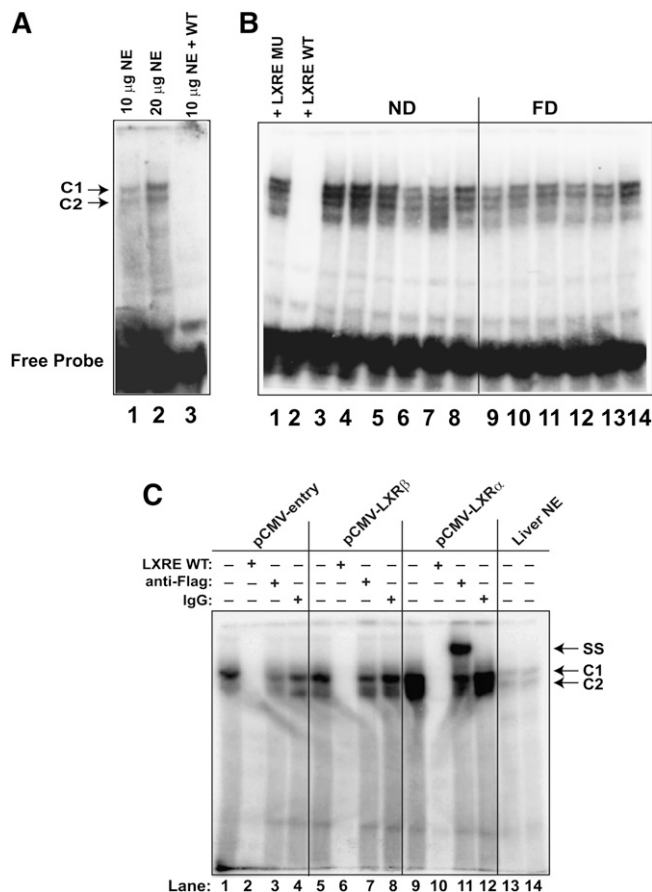
Fig. 6. Reduced bindings of FD nuclear extracts to ACSL3-LXRE sequence. (A) A double-stranded oligonucleotide (LXRE-wt) corresponding to hamster ACSL3 promoter region −191 to −156 was ^{32}P-labeled and incubated with 10 or 20 µg of nuclear extracts of a ND hamster liver in the absence (lanes 1 and 2) or presence of 100-fold of unlabeled LXRE-wt probe (lane 3). (B) ACSL3-LXRE-labeled probe was incubated with 25 µg of ND hamster liver tissue nuclear extracts (lanes 1–8) and FD group (lanes 9–14) for 10 min at 22°C. In lanes 1 and 2, a ND nuclear extract was incubated with ^{32}P-labeled probe in the presence of either unlabeled mutated LXRE or the unlabeled wt probe to demonstrate the binding specificity. (C) Nuclear extracts were prepared from HEK293 cells that had been transfected with indicated plasmids. EMSA in the absence or the presence of anti-Flag or IgG was conducted as described in (A).

mRNA levels of ACSL3 and ABCA1, an authentic LXR target gene (39). Activation of LXR by the agonist increased ACSL3 mRNA expression to a similar extent as the induction of ABCA1 in primary hepatocytes (**Fig. 7A**). Next, we examined the effects of the siRNA-mediated knockdown of LXRα and LXRβ on ACSL3 and ABCA1 gene expression in HepG2 cells that were either untreated or treated with GW3965. Transfection of specific siRNAs reduced endogenous mRNA expression of LXRα and LXRβ by approximately 60% relative to what was caused by a nonspecific siRNA with a scrambled sequence (Fig. 7B). Importantly, transfection of siLXRα into HepG2 cells reduced the agonist-induced ACSL3 gene expression (Fig. 7C) from 2.5- to 1.2-fold. Cotransfection of si-LXRα and si-LXRβ resulted in a complete loss of the ligand induction of ACSL3 mRNA expression without reducing the basal ACSL3 mRNA

level. We observed an almost identical pattern in the loss of ligand-induced elevation in ABCA1 mRNA expression by the siRNA targeted knockdown of LXRs in HepG2 cells (Fig. 7D).

Effects of diet and LXR ligand activation on serum and hepatic lipid levels of hamsters

To further examine the function and the specificity of LXR in the regulation of hepatic ACSL3 expression in hamsters under normolipidemic and dyslipidemic conditions, hamsters were fed ND or FD for two weeks and were subsequently orally dosed by GW3965 (30 mg/kg) or the vehicle for seven days. Fasting serum was collected before and after the treatment, and food intake and body weight were recorded daily. In addition, liver weights were measured at the termination.

The food intake and body weights were not significantly different between the FD and ND groups with vehicle or with GW3965 treatment (supplementary Fig. IIA, B). The liver weights in FD vehicle group were 30% higher than the ND vehicle group ($P < 0.01$), and GW3965 treatment did not significantly increase liver weights of either diet group (supplementary Fig. IIC). Serum TC levels were increased approximately 35% ($P < 0.01$) by FD, and GW compound did not significantly affect serum TC levels in FD and ND groups (**Fig. 8A**). However, different from the effect on TC, the fructose-induced elevation of serum TG level (2.2-fold of ND, $P < 0.01$) was further increased 85% ($P < 0.001$) by GW3965 (Fig. 8A). The effects of GW3965 on serum triglycerides have been previously reported in hamsters (40, 41) and other rodent models (42).

We extracted lipids from all liver samples and measured cholesterol and triglyceride levels (Fig. 8B). We did not detect changes in liver cholesterol levels between FD and ND groups in vehicle-treated hamsters, whereas GW3965 increased liver cholesterol content in fructose-fed hamsters. Interestingly, hepatic triglyceride levels were substantially lowered by GW3965 in both ND and FD groups. The lipid extraction and measurements were repeated, and we obtained the same results.

Activation of LXR by GW3965 increases hepatic ACSL3 expression in hamsters

We isolated RNA and analyzed ACSL mRNA expressions in all liver samples. qPCR results showed that in ND group, the level of ACSL3 mRNA was increased approximately 47% ($P < 0.001$) by ligand treatment compared with vehicle control (**Fig. 9A**). The reduction of ACSL3 gene expression by fructose was blunted by GW compound. Importantly, the mRNA levels of ACSL1, ACSL4, and ACSL5 were not affected by the ligand treatment or by fructose diet, thereby further confirming the specific effect of LXR activation on isozyme ACSL3 gene transcription in liver tissue. Furthermore, we examined levels of ACSL3 and ACSL1 proteins among liver samples of the four groups by Western blot analysis. As shown in Fig. 9B, ACSL3 protein abundance was increased 70% ($P < 0.05$) by GW3965 in hamster livers of normal diet. Fructose diet lowered ACSL3 protein amount compared with ND group, and ligand treatment
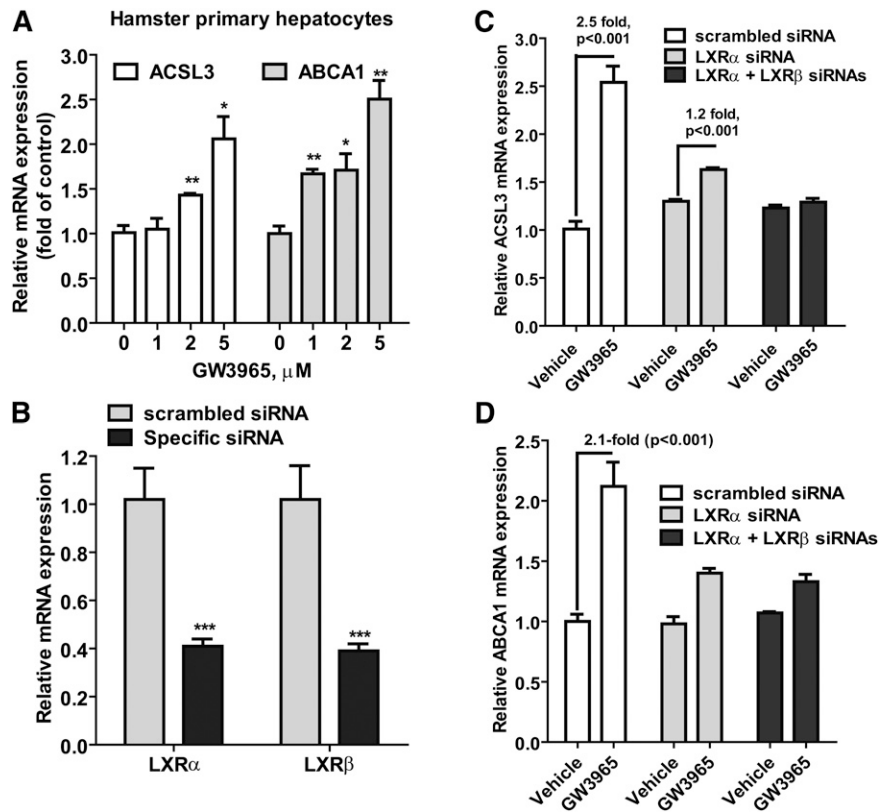
Fig. 7. LXR-dependent induction of ACSL3 gene expression in hamster primary hepatocytes and HepG2 cells. (A) Hamster primary hepatocytes were cultured in HepatoZYME-SFM medium overnight. GW3965 at indicated concentrations were added to the cells for 24 h before the isolation of total RNA. Real-time qPCR assays were conducted to examine ACSL3 and ABCA1mRNA levels of untreated and treated samples. (B) Specific siRNAs and scrambled siRNA were individually transfected into HepG2 cells in 6-well plates. Two days after transfection, total RNA was isolated, and cDNA was synthesized from total RNA. LXRα, LXRβ, and GAPDH mRNA levels were measured by q-PCR, and relative mRNA levels are presented. (C and D) After siRNA transfections, cells were treated with 5 μM of GW3965 for 24 h before cell lysis for total RNA isolations and qPCR analysis of mRNA levels of ACSL3 (C) and ABCA1 (D). Data shown are representative of two separate siRNA transfections that had similar results.

raised the ACSL3 protein amount. However, we could not accurately quantify the ligand effect in FD groups due to the low signals. In contrast to ACSL3, ACSL1 protein remained unchanged among the four groups. These results reassured the specific inductive effect of GW3965 and the suppressive effect of fructose on ACSL3 mRNA expressions in hamster liver.

In addition to ACSL family, we performed qPCR analysis to examine changes in mRNA levels of LXRs. Similar to our first FD study described in Fig. 4, the mRNA levels of LXRα, LXRβ, and RXRβ were not affected by ligand activation, but they were reduced by FD (Fig. 9C). To further confirm the lack of effect of FD on gene expression of PPARs, we measured the mRNA levels of PPARs in all liver samples, and no significant differences between diet groups or treatment groups were found (Fig. 9D).

DISCUSSION

High-fructose diets have been demonstrated to cause hypertriglyceridemia and hepatic steatosis. Several major transcriptional networks have been shown to be dysregulated by fructose-enriched diets, such as SREBP pathway and ChREBP pathway (35–37), resulting in the induction of de novo lipogenesis as well as gluconeogenesis in liver tissue. In this study, we identified that the LXR signaling pathway is significantly downregulated by fructose diet in hamster liver, leading to the substantially reduced expression and activity of ACSL3, a cellular enzyme that has critical roles in fatty acid metabolism.

With the exception of ACSL6, all ACSL isozymes are expressed in the liver. ACSL1 is the most abundant isoform in liver tissue, and it was originally thought to play pivotal role in hepatic TAG synthesis and FA β-oxidation (8, 43). However, the recent study of liver-specific knockout of ACSL1 in mice revealed only minor defects in both hepatic FA oxidation and TG synthesis (11). The lack of impact of depletion of ACSL1 on lipid metabolism in the liver suggests that other ACSL isoforms may be prominently involved in liver FA metabolism, despite being less abundant in liver tissue.

Our investigation initially set out to determine whether a dyslipidemic fructose diet could affect the expression of ACSL family members in an isoform-specific manner, with the hope that such a study would provide new insight into
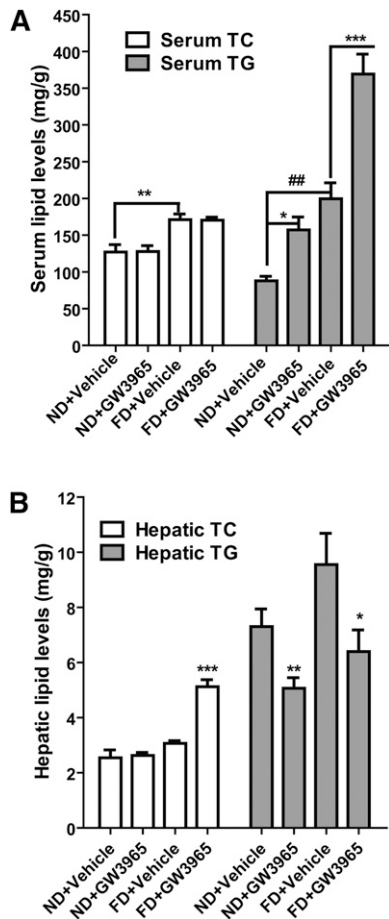
Fig. 8. Effects of GW3965 on serum and hepatic lipid levels. Thirty-six hamsters were divided into four groups (n = 8 per group). Groups 1 and 2 were fed ND and groups 3 and 4 were fed FD for two weeks. Hamsters were either treated with 30 mg/kg of GW3965 or with vehicle for seven days. (A) TC and TG levels in hamster sera were measured after treatment with GW3965 or vehicle. Data are mean ± SEM of eight hamsters per group. *$P < 0.05$, **$P < 0.01$, and ***$P < 0.001$ for comparing differences between GW3965 and vehicle; ##$P < 0.01$ for comparing differences between FD and ND without ligand treatment. (B) TC and TG levels were measured in all liver samples. Data are mean ± SEM (n = 8). *$P < 0.05$, **$P < 0.01$, and ***$P < 0.001$ compared with vehicle group.

the underlying mechanisms that regulate the transcription of ACSL under pathological conditions. Indeed, the current results of our ACSL profiling at both mRNA and protein levels revealed that only ACSL3 expression was markedly reduced by the fructose diet. Our enzyme assays utilizing three different FA substrates further showed that the enzyme-catalyzed synthesis of palmitoyl-CoA was not altered after feeding fructose diet, which was consistent with the unchanged expression of ACSL1, which prefers palmitic acid and other saturated FAs as substrates. In contrast, enzymatic activities in synthesizing arachidonoyl-CoA and oleoyl-CoA were both reduced by approximately 22% and 30%, respectively, after feeding fructose diet. Because ACSL3 is not the most abundant ACSL isozyme in the liver and other ACSL isoforms in the liver, particularly ACSL4, also preferred unsaturated FAs as substrates (14), this modest reduction in total ACSL enzyme activity seemed important.

The PPAR family of nuclear receptors is known to play a major role in the transcriptional regulation of ACSL family members. Particularly, PPARδ is a strong activator of ACSL3 gene transcription in liver cells (21). Surprisingly, the decrease of ACSL3 expression was not associated with a reduction of PPARδ expression or activity by fructose diet. Although we observed a small decrease in PPARα mRNA level in livers of FD hamsters in our first fructose diet study, we did not observe this reduction again from the repeated fructose diet study. Utilizing freshly isolated hamster hepatocytes, we also demonstrated that activation of PPARα increased ACSL1 without affecting ACSL3 expression. Altogether, these results ruled out the involvement of PPARα in the FD-mediated suppression of ACSL3 transcription. It is noteworthy that these new data generated from hamster liver tissue and hepatocytes provided additional evidence supporting our hypothesis that ACSL family members are distinctly regulated by individual PPAR nuclear receptors in a PPAR isotype-specific matter.

In contrast to the lack of significant changes in PPARs, we observed a strong correlation between the reduction of ACSL3 and the decreased expression of three major LXR nuclear receptors, LXRα, LXRβ, and RXRβ, in livers of FD hamsters. The results of EMSA further demonstrated the reduced binding of LXR/RXR to the identified ACSL3-LXRE sequence motif of the hamster ACSL3 gene promoter from nuclear extracts of FD hamsters compared with liver extracts of ND hamsters. The EMSA detected two major complexes, C1 and C2. Through transient transfections of Flag-tagged LXRα and LXRβ into HEK293 cells and supershift assays, we obtained primary evidence showing that LXRα was predominantly present in C1 and C2, and it possibly forms different heterodimers with RXRα/β.

In this study, we conducted three different lines of investigation to demonstrate the specific effect of LXR activation on ACSL3 gene expression in liver cells. First, we demonstrated that the promoter activity of hamster ACSL3 gene is activated by GW3965, a specific LXR agonist, in LXRE- and LXR-dependent fashions. Second, siRNA-mediated reductions of LXRα/β in HepG2 cells nearly abolished the GW3965-induced ACSL3 gene expression without a significant impact on the basal level of ACSL3 mRNA. It is possible that the basal transcription of ACSL3 in HepG2 cells is primarily regulated by PPARδ, which would not be affected by siRNAs targeted to LXRs. Third, we provided strong in vivo evidence demonstrating that administration of GW3965 to hamsters only increased ACSL3 mRNA and protein expressions without effects on other liver-expressed ACSL isoforms.

Previous studies using LXR agonists, including GW3965, reported inconsistent results of the effects of LXR activation on hepatic triglyceride levels. In one study of hamster fed a normal diet, GW3965 treatment of 7 days at 30 mg/kg dose increased serum TG, but it did not change hepatic triglyceride levels (40). By utilizing LDL receptor knockout mice, Quinet et al. reported that 10 mg/kg dose of GW3965 did not affect serum or hepatic TG levels, whereas another LXR agonist (LXR-623) significantly reduced
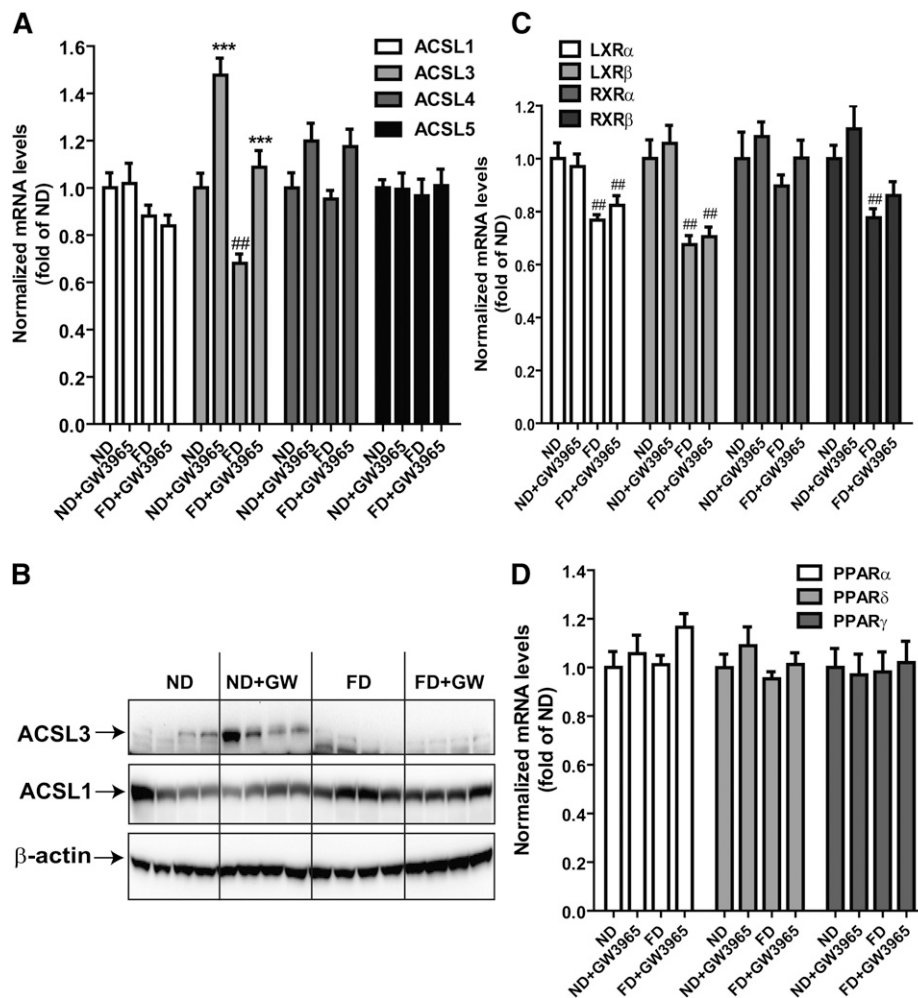
Fig. 9. Induction of ACSL3 expression in hamster liver by GW3965 treatment. Hamsters were euthanized, and liver tissues were isolated at the end of treatment. (A, C, and D) Total RNA was isolated from each liver sample and relative mRNA abundances of indicated genes were determined by conducting real-time PCR and normalized to GAPDH. ***$P < 0.001$ compared with vehicle group of the same diet; ##$P < 0.01$ compared with vehicle ND group. (B) Total protein extracts were individually prepared from four randomly chosen liver samples from each group. Equal amounts of homogenate proteins (50 µg) were resolved by SDS-PAGE and ACSL3, and ACSL1 proteins were detected by immunoblotting using anti-ACSL3 antibody or anti-ACSL1 antibody. The membrane was reprobed with an anti-β-actin antibody.

hepatic triglyceride levels (42). Moreover, in a recent study to examine the effects of LXR activation on reverse cholesterol transport in hamsters fed a rodent diet containing 0.3% cholesterol, GW3965 treatment of 10 days at the same 30 mg/kg dose did not alter hepatic cholesterol or triglyceride levels (41). In the current study, we observed a strong reduction of hepatic triglyceride levels in both ND and FD groups. We repeated the whole-lipid extractions and measurements, and we obtained same results. Currently, we do not fully understand the discrepancies between our studies and some of previously reported ones. In addition, GW3965 treatment increased serum TG in both diet groups. It is not clear whether the reduction of hepatic TG was linked to the increase in serum TG by GW3965 administration. It is also quite possible that some other aspects of hepatic lipid metabolism, such as lipoprotein uptake through LDL receptor- or VLDL receptor-mediated events, were altered by LXR activation.

Additional investigations are needed to examine the effects of GW3965 on those aspects for a comprehensive understanding of the altered lipid metabolism in hamsters after administration of LXR agonist.

Previous studies of ACSL3 function by different investigators have yielded different results in relation to FA metabolism in liver cells and other cell types. ACSL3 has been identified as a protein associated with lipid droplets (44). A recent study further showed that ACSL3 has a function in local lipid synthesis (45). In that study, increased ACSL3 expression in COS-7 cells led to increased fatty acid uptake. Conversely, depletion of ACSL3 lowered FA uptake in COS-7 cells. Studies in rat primary hepatocytes suggested a role of ACSL3 in directing FAs into the TG anabolic pathway (46). On the other hand, we showed recently that the overexpression of ACSL3 in hamster liver through adenovirus-mediated gene delivery resulted in reductions of serum and hepatic TG (47). In the current study, the

GW3965-stimulated increases in ACSL3 expression in liver were associated with reductions of hepatic triglyceride levels, which are consistent with the observation of reduced ACSL3 expression/activity by fructose feeding and a tendency of induction of triglyceride accumulation by fructose diet in hamster liver. Altogether, our hamster studies suggest that ACSL3 may have an important function in directing hepatic FA entry into the catabolic pathway to reduce triglyceride accumulation in liver tissue.

REFERENCES

1. Faergeman, N. J., and J. Knudsen. 1997. Role of long-chain fatty acyl-coA esters in the regulation of metabolism and in cell signaling. *Biochem. J.* **323:** 1–12.
2. Coleman, R. A., T. M. Lewin, C. G. Van Horn, and M. R. Gonzalez-Baro. 2002. Do acyl-CoA synthetases regulate fatty acid entry into synthetic versus degradative pathways? *J. Nutr.* **132:** 2123–2126.
3. Soupene, E., and F. A. Kuypers. 2008. Mammalian long-chain acyl-CoA synthetases. *Exp. Biol. Med. (Maywood).* **233:** 507–521.
4. Mashek, D. G., and R. A. Coleman. 2007. Long-chain acyl-CoA synthetases and fatty acid channeling. *Future Lipidol.* **2:** 465–476.
5. Ellis, J. M., J. L. Frahm, L. O. Li, and R. A. Coleman. 2010. Acyl-coenzyme A synthetases in metabolic control. *Curr. Opin. Lipidol.* **21:** 212–217.
6. Lewin, T. M., and C. G. Van Horn. 2002. Rat liver acyl-CoA synthetase 4 is a peripheral-membrane protein located in two distinct subcellular organelles, peroxisomes, and mitochondrial-associated membrane. *Arch. Biochem. Biophys.* **404:** 263–270.
7. Lobo, S., B. M. Wiczer, and D. A. Bernlohr. 2009. Functional analysis of long-chain acyl-CoA synthetase 1 in 3T3–L1 adipocytes. *J. Biol. Chem.* **284:** 18347–18356.
8. Parkes, H. A., E. Preston, D. Wilks, M. Ballesteros, L. Carpenter, L. Wood, E. W. Kraegen, S. M. Furler, and G. J. Cooney. 2006. Overexpression of acyl-CoA synthetase-1 increases lipid deposition in hepatic (HepG2) cells and rodent liver in vivo. *Am. J. Physiol. Endocrinol. Metab.* **291:** E737–E744.
9. Durgan, D. J., J. K. Smith, M. A. Hotze, O. Egbejimi, K. D. Cuthbert, V. G. Zaha, J. R. B. Dyck, E. D. Abel, and M. E. Young. 2006. Distinct transcriptional regulation of long-chain acyl-CoA synthetase isoforms and cytosolic thioesterase 1 in the rodent heart by fatty acids and insulin. *Am. J. Physiol. Heart Circ. Physiol.* **290:** H2480–H2497.
10. Marszalek, J. R., C. Ktidis, A. Dararutana, and H. F. Lodish. 2004. Acyl-coA synthetase 2 (ACSL2) over expression enhances fatty acid internalization and neurite outgrowth. *J. Biol. Chem.* **279:** 23882–23891.
11. Li, L. O., J. M. Ellis, H. A. Paich, S. Wang, N. Gong, G. Altshuller, R. J. Thresher, T. R. Koves, S. M. Watkins, D. M. Muoio, et al. 2009. Liver-specific loss of long chain acyl-CoA synthetase-1 decreases triacylglycerol synthesis and beta-oxidation and alters phospholipid fatty acid composition. *J. Biol. Chem.* **284:** 27816–27826.
12. Ellis, J. M., O. L. Li, P-C. Wu, T. R. Koves, O. I. Ikayeva, R. D. Stevens, S. M. Watkins, D. M. Muoio, and R. A. Coleman. 2010. Adipose acyl-CoA synthetase-1 directs fatty acids toward β-oxidation and is required for cold thermogenesis. *Cell Metab.* **12:** 53–64.
13. Ellis, J. M., S. M. Mentock, M. A. DePetrillo, T. R. Koves, S. Sen, S. M. Watkins, D. M. Muoio, G. W. Cline, H. Taegtmeyer, G. I. Shulman, et al. 2011. Mouse cardiac acyl coenzyme A synthetase 1 deficiency impairs fatty acid oxidation and induces cardiac hypertrophy. *Mol. Cell. Biol.* **31:** 1252–1262.
14. Golej, D. L., B. Askari, F. Kraemer, S. Barnhart, A. Vivekanandan-Giri, S. Pennathur, and K. E. Bornfeldt. 2011. Long-chain acyl-CoA synthetase 4 modulates prostaglandin E2 release from human arterial smooth muscle cells. *J. Lipid Res.* **52:** 782–793.
15. Mashek, D. G., L. O. Li, and R. A. Coleman. 2006. Rat long-chain acyl-CoA synthetase mRNA, protein, and activity vary in tissue distribution and in response to diet. *J. Lipid Res.* **47:** 2004–2010.
16. Wu, M., H. Liu, W. Chen, Y. Fujimoto, and J. Liu. 2009. Hepatic expression of long-chain acyl-CoA synthetase 3 is upregulated in hyperlipidemic hamsters. *Lipids.* **44:** 989–998.
17. Achouri, Y., B. D. Hegarty, D. Allanic, D. Becard, I. Hainault, and F. Foufelle. 2005. Long chain fatty acyl-CoA synthetase 5 expression is induced by insulin and glucose: involvement of sterol regulatory element-binding protein-1c. *Biochimie.* **87:** 1149–1155.
18. Schoonjans, K., M. Watanabe, H. Suzuki, A. Mahfoudi, G. Krey, W. Wahli, P. Grimaldi, B. Staels, T. Yamamoto, and J. Auwerx. 1995. Induction of the acyl-coenzyme A synthetase gene by fibrates and fatty acids is mediated by a peroxisome proliferator response element in the C promoter. *J. Biol. Chem.* **270:** 19269–19276.
19. Martin, G., K. Schoonjans, A-M. Lefebvre, B. Staels, and J. Auwerx. 1997. Coordinate regulation of the expression of the fatty acid transport protein and acyl-CoA synthetase genes by PPARα and PPARγ activators. *J. Biol. Chem.* **272:** 28210–28217.
20. Gerhold, D. L., F. Liu, G. Jiang, Z. Li, J. Xu, M. Lu, J. R. Sachs, A. Bagchi, A. Fridman, and D. J. Holder. 2002. Gene expression profile of adipocyte differentiation and its regulation by peroxisome proliferator-activated receptor-gamma agonists. *Endocrinology.* **143:** 2106–2118.
21. Cao, A., H. Li, Y. Zhou, M. Wu, and J. Liu. 2010. Long chain acyl-CoA synthetase-3 is a molecular target for peroxisome proliferator-activated receptor δ in HepG2 hepatoma cells. *J. Biol. Chem.* **285:** 16664–16674.
22. Apfel, R., D. Benbrook, E. Lernhardt, M. A. Ortiz, G. Salbert, and M. Pfahl. 1994. A novel orphan receptor specific for a subset of thyroid hormone-responsive elements and its interaction with the retinoid/thyroid hormone receptor subfamily. *Mol. Cell. Bio.* **14:** 7025–7035.
23. Boergesen, M., T. A. Pedersen, B. Gross, S. J. van Heeinggen, D. Hagenbeek, C. Bindesboll, S. Caron, F. Lalloyer, K. R. Steffensen, H. I. Nebb, et al. 2012. Genome-wide profiling of liver-X receptor, retinoid X receptor, and peroxisome proliferator-activated receptor α in mouse liver reveals extensive sharing of binding sites. *Mol. Cell. Biol.* **32:** 852–867.
24. Dawson, M. I., and Z. Xia. 2012. The retinoid X receptors and their ligands. *Biochim. Biophys. Acta.* **1821:** 21–56.
25. Jakobsson, T., E. Treuter, J. A. Gustafsson, and K. R. Steffensen. 2012. Liver X receptor biology and pharmacology: new pathways, challenges and opportunities. *Trends Pharmacol. Sci.* **33:** 394–404.
26. Maxwell, K. N., R. E. Soccio, E. M. Duncan, E. Sehayek, and J. L. Reslow. 2003. Novel putative SREBP and LXR target genes identified by microarray analysis in liver of cholesterol-fed mice. *J. Lipid Res.* **44:** 2109–2119.
27. Weedon-Fekjaer, M. S., K. T. Dalen, K. Solaas, A. C. Staff, A. K. Dutaroy, and H. I. Nebb. 2010. Activation of LXR increases acyl-CoA synthetase activity through direct regulation of ACSL3 in human placental trophoblast cells. *J. Lipid Res.* **51:** 1886–1896.
28. Srivastava, R. A. K. 2011. Evaluation of anti-atheroclerotic activities of PPARα, PPARγ, and LXR agonists in hyperlipidemic atherosclerosis-susceptible F1B hamsters. *Atherosclerosis.* **214:** 86–93.
29. Srivastava, R. A., and S. He. 2010. Anti-hyperlipidemic and insulin sensitizing activities of fenofibrate reduces aortic lipid deposition in hyperlipidemic Golden Syrian hamster. *Mol. Cell. Biochem.* **345:** 197–206.
30. Ohtani, H., K. Hayashi, Y. Hirata, S. Dojo, K. Nakashima, E. Nishio, H. Kurushima, M. Saeki, and G. Kajiyama. 1990. Effects of dietary cholesterol and fatty acids on plasma cholesterol level and hepatic lipoprotein metabolism. *J. Lipid Res.* **31:** 1413–1422.
31. Liu, G., L. Fan, and R. Redinger. 1991. The association of hepatic apolipoprotein and lipid metabolism in hamsters and rats. *Comp. Biochem. Physiol. A. Comp. Physiol.* **99:** 223–228.
32. Sullivan, M. P., J. J. Cerda, F. L. Robbins, C. W. Burgin, and R. J. Beatty. 1993. The gerbil, hamster, and guinea pig as rodent models for hyperlipidemia. *Lab. Anim. Sci.* **43:** 575–578.
33. Dong, B., M. Wu, H. Li, F. B. Kraemer, K. Adeli, N. G. Seidah, S. W. Park, and J. Liu. 2010. Strong induction of PCSK9 gene expression through HNF1α and SREBP2: Mechanism for the resistance to LDL-cholesterol lowering effect of statins in dyslipidemic hamsters. *J. Lipid Res.* **51:** 1486–1495.
34. Basciano, H., E. M. Abigale, M. Naples, C. Baker, R. Kohen, E. Xu, Q. Su, E. M. Allister, M. B. Michael, and K. Adeli. 2009. Metabolic effects of dietary cholesterol in an animal model of insulin resistance and hepatic steatosis. *Am. J. Physiol. Endocrinol. Metab.* **297:** E462–E473.
35. Koo, H. Y., M. A. Wallig, B. H. Chung, T. Y. Nara, B. H. Cho, and M. T. Nakamura. 2008. Dietary fructose induces a wide range of genes with distinct shift in carbohydrate and lipid metabolism in fed and fasted rat liver. *Biochim. Biophys. Acta.* **1782:** 341–348.
36. Koo, H. Y., M. Miyashita, B. H. Cho, and M. T. Nakamura. 2009. Replacing dietary glucose with fructose increases ChREBP activity

and SREBP-1 protein in rat liver nucleus. *Biochem. Biophys. Res. Commun.* **390:** 285–289.

37. Tappy, L., and K. A. Le. 2010. Metabolic effects of fructose and the worldwide increase in obesity. *Physiol. Rev.* **90:** 23–46.

38. Fujino, T., M. J. Kang, H. Suzuki, H. Iijima, and T. Yamamoto. 1996. Molecular characterization and expression of rat acyl-CoA synthetase 3. *J. Biol. Chem.* **271:** 16748–16752.

39. Yvan-Charvet, L., M. Ranalletta, N. Wang, S. Han, N. Terasaka, R. Li, C. Wesch, and A. R. Tall. 2007. Combined deficiency of ABCA1 and ABCG1 promotes foam cell accumulation and accelerates atherosclerosis in mice. *J. Clin. Invest.* **117:** 3900–3908.

40. Groot, P. H., N. J. Pearce, J. W. Yates, C. Stocker, C. Sauermelch, C. P. Doe, R. N. Willette, A. Olzinski, T. Peters, D. d'Epagnier, et al. 2005. Synthetic LXR agonists increase LDL in CETP species. *J. Lipid Res.* **46:** 2182–2191.

41. Briand, F., M. Treguier, A. Andre, D. Grillot, M. Issandou, K. Ouguerram, and T. Sulpice. 2010. Liver X receptor activation promotes macrophage-to-feces reverse cholesterol transport in a dyslipidemic hamster model. *J. Lipid Res.* **51:** 763–770.

42. Quinet, E. M., M. D. Basso, A. R. Halpern, D. W. Yates, R. J. Steffan, V. Clerin, C. Resmini, J. C. Keith, T. J. Berrodin, I. Feingold, et al. 2009. LXR ligand lowers LDL cholesterol in primates, is lipid neutral in hamster, and reduces atherosclerosis in mouse. *J. Lipid Res.* **50:** 2358–2370.

43. Li, L. O., D. G. Mashek, J. An, S. D. Doughman, C. B. Newgard, and R. A. Coleman. 2006. Overexpression of rat long chain acyl-CoA synthetase 1 alters fatty acid metabolism in rat primary hepatocytes. *J. Biol. Chem.* **281:** 37246–37255.

44. Brasaemle, D. L., G. Dolios, L. Shapiro, and R. Wang. 2004. Proteomic analysis of proteins associated with lipid droplets of basal and lipolytically stimulated 3T3-L1 adipocytes. *J. Biol. Chem.* **279:** 46835–46842.

45. Poppelreuther, M., B. Rudolph, C. Du, R. Großmann, M. Becker, C. Thiele, R. Ehehalt, and J. Füllekrug. 2012. The N-terminal region of acyl-CoA synthetase 3 is essential for both the localizationon lipid droplets and the function in fatty acid uptake. *J. Lipid Res.* **53:** 888–900.

46. Bu, S. Y., M. T. Mashek, and D. G. Mashek. 2009. Suppression of long chain acyl-CoA synthetase 3 decreases hepatic de novo fatty acid synthesis through decreased transcriptional activity. *J. Biol. Chem.* **284:** 30474–30483.

47. Wu, M., A. Cao, B. Dong, and J. Liu. 2011. Reduction of serum free fatty acids and triglycerides by liver-targeted expression of long chain acyl-CoA synthetase 3. *Int. J. Mol. Med.* **27:** 655–662.